direction of the Poynting vector shows more clearly transient characteristics of the directional coupler by presenting the pattern of the flow of the electromagnetic energy.

IV. Conclusion

The time variation of electromagnetic fields can be described in two ways. Either the instantaneous distribution is shown or the spatial distribution obtained by taking the envelope of the maximum value during the observation time interval is shown. Using the former method, for example, the detailed propagation characteristics such as the phase and the amplitude of the coupled microstrip slotline at each mode is known. Using the latter method, the process by which the stationary property of the directional coupler is brought about can be known. Also, the expression of the time variation of the instantaneous distribution and the Poynting vector shows more clearly the transient characteristics of the complicated circuit elements, such as the directional coupler. These can be realized by using all electromagnetic components. As shown in this paper, this condition is satisfied by the present method.

In addition, we can easily study the time variations of field in the case of pulse waves where the analysis of the transient phenomena is very important. More analysis is needed for when the size of the slot becomes less, Z_{even} increases, and Z_{odd} decreases, so that a higher coupling directional coupler can be obtained. This subject and results of the pulse wave analysis will be reported in a later paper.

References

[1] F. C. de Ronde, "A new class of microstrip directional coupler," *IEEE Trans Microwave Theory Tech.*, vol. MTT-18, pp. 184–186, May 1970.

[2] B. Schiek, "Hybrid branch line couplers—A useful class of directional couplers," *IEEE Trans. Microwave Theory Tech.*, vol. MTT-22, pp. 864–869, Oct. 1974.

[3] B. Schiek and J. Köhler, "Improving the isolation of 3-dB couplers in microstrip-slotline technique," *IEEE Trans. Microwave Theory Tech.*, vol. MTT-26, pp. 5–7, Jan. 1978.

[4] H. Ogawa, T. Hirota, and M. Aikawa, "Coupled microstrip-slotline directional coupler," *Trans.IECE Japan*, vol. J65-B, pp. 882–889, July 1982.

[5] M Aikawa, "Microstrip line directional coupler with tight coupling and high directivity," *Trans IECE Japan*, vol. J60-B, pp. 253–259, Apr. 1977.

[6] R. K. Hoffmann and J. Siegl, "Microstrip-slot coupler design—Part I: S-parameters of uncompensated and compensated couplers," *IEEE Trans. Microwave Theory Tech.*, vol. MTT-30, pp 1205–1210, Aug. 1982.

[7] R. K. Hoffmann and J. Siegl, "Microstrip-slot coupler design—Part II: Practical design aspects," *IEEE Trans. Microwave Theory Tech.*, vol. MTT-30, pp. 1211–1216, Aug. 1982.

[8] S. Koike, N. Yoshida, and I. Fukai, "Transient analysis of microstrip gap," *Electron. Commun. Japan*, vol. 67-B, pp. 76–83, Nov. 1984.

[9] S. Koike, N. Yoshida, and I. Fukai, "Transient analysis of microstrip gap in three-dimensional space," *IEEE Trans. Microwave Theory Tech.*, vol. MTT-33, pp. 726–730, Aug 1985.

[10] S. Koike, N. Yoshida, and I. Fukai, "Transient analysis of coupled microstrip-slotline," *Trans. IECE Japan*, vol. J68-B, pp. 811–818, July 1985.

[11] N. Yoshida and I. Fukai, "Transient analysis of a stripline having a corner in three-dimensional space," *IEEE Trans. Microwave Theory Tech.*, vol. MTT-32, pp. 491–498, May 1984.

[12] S Akhtarzad and P. B Johns, "Solution of Maxwell's equations in three space dimensions and time by the t.l.m. method of numerical analysis," *Proc. Inst. Elec. Eng.*, vol. 122, pp. 1344–1348, Dec. 1975.

[13] T. Itoh and R. Mittra, "Spectral-domain approach for calculating the dispersion characteristics of microstrip lines," *IEEE Trans. Microwave Theory Tech.*, vol. MTT-21, pp. 496–499, July 1973

[14] H. A. Wheeler, "Transmission-line properties of a strip on a dielectric sheet on a plane," *IEEE Trans. Microwave Theory Tech* , vol. MTT-25, pp. 631–647, Aug. 1977.

[15] S. B. Cohn, "Slot line on a dielectric substrate," *IEEE Trans. Microwave Theory Tech.*, vol. MTT-17, pp. 768–778, Oct. 1969.

Focused Heating in Cylindrical Targets—Part II

JAMES R. WAIT, FELLOW, IEEE, AND MIKAYA LUMORI

***Abstract*—We implement the analytical formulation for the local power dissipated in a conductive target of cylindrical form that was described in Part I. The scheme employs a number N of horn apertures arranged around the periphery of the target. We show sample results for the radial and the azimuthal variations of the normalized local power. The cases where the array is focused at both the center of the target and where it is focused at an eccentric point are considered for $N = 4$, 8, and 16. It is shown that the unwanted secondary "hot spots" can be eliminated if the number N of horn apertures is increased sufficiently. The results are relevant to microwave thermic heating in cancer therapy.**

I. Introduction

The formulation given in a previous communication on focused heating [1] in a cylindrical conductor has now been implemented numerically. The scheme involves placing N aperture sources around the periphery of the target. In our example here, we have chosen $N = 4$, 8, and 16. The formulation follows that in Part I, but we now normalize the results for the purpose of graphical presentation. Finally, we draw some general conclusions about the nature of electromagnetic heating in hyperthermia.

II. Description of the Model

The assumed geometry of the configuration is purely two dimensional, as described quite fully in Part I. The cylindrical target of radius a is homogeneous with conductivity σ, permittivity ϵ, and the free-space permeability μ_0. The horn apertures are disposed around the periphery, arranged so that no gaps exist between them. As indicated in [1, fig. 1] the center of each aperture is located at $\phi_n = n\pi/N$, where $n = 0,1,2,\cdots N-1$.

Because of the assumed polarization of the excitation, the electric field in the target has only an axial or z component, which is written conveniently in the form

$$E_z(\rho,\phi) = \sum_{n=0}^{N-1} E_{z,n}(\rho,\phi).$$

Here

$$E_{z,n}(\rho,\phi) = \Delta_n e^{i\delta_n} \sum_{m=-\infty}^{+\infty} A_m I_m(\gamma\rho)\, e^{-im(\phi-\phi_n)}$$

is the field produced by the nth aperture, where A_m is a coefficient, $I_m(\gamma_\rho)$ is the modified Bessel function of argument $\gamma\rho$, and γ is the complex propagation constant of the homogeneous interior of the target. We recall that $\gamma = [i\mu_0\omega(\sigma + i\epsilon\omega)]^{1/2}$ for a time factor $\exp(i\omega t)$.

Each aperture is assumed to have the same field distribution (as a function of ϕ), but the relative amplitude Δ_n and phase δ_n of each aperture are controllable. For the results presented here, we assume that the horn apertures are in direct contact with the target (i.e., $b = a$ in [1, fig. 1]). Thus, we can write

$$A_m = \frac{1}{2\pi I_m(\gamma a)} \int_{-\pi/N}^{\pi/N} E_{z,0}(a,\phi)\, e^{im\phi}\, d\phi$$

where $E_{z,0}(a,\phi)$ is the aperture illumination over the reference

Manuscript received May 17, 1985, revised October 21, 1985.

The authors are with the Electromagnetics Laboratory, Department of Electrical and Computer Engineering, University of Arizona, Tucson, AZ 85721.

IEEE Log Number 8406857.

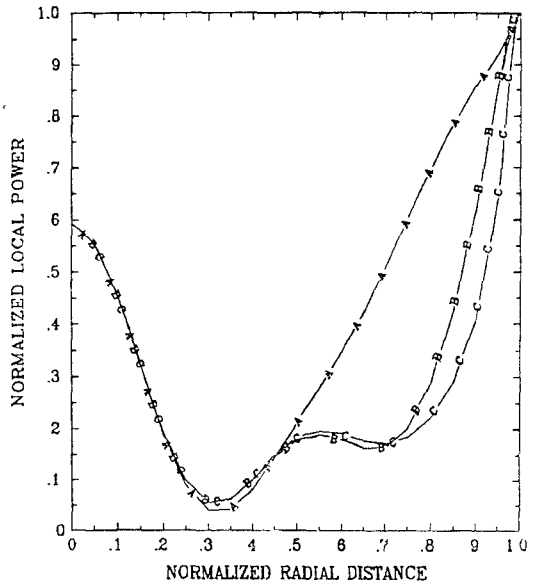

Fig. 1 Local power dissipation as a function of radial coordinate for the aperture array focused at the center of the conductive cylindrical target. Curve A for $N=4$ apertures, B for $N=8$, and C for $N=16$.

horn at $\phi=\phi_0=0^0$. In accordance with Part I, we choose

$$E_{z,0}(a,\phi)=E_{z,0}(a,0)\cos(N\phi/2)$$
$$\text{for } -\pi/N<\phi<+\pi/N$$

where

$$E_{z,0}=E_0\cdot\Delta_0\cdot e^{i\delta_0}.$$

Thus, we find without difficulty that

$$2\pi I_m(\gamma a)A_m = \left[\frac{E_0 N}{(N/2)^2-m^2}\right]\cos(m\pi/N), \qquad m\neq N/2$$
$$= E_0\pi/N, \qquad m=N/2.$$

Now the local power dissipation at the point (ρ,ϕ) in the target is $\sigma|E_z(\rho,\phi)|^2$ in W/m^3, where σ is the conductivity. To facilitate the presentation, we define a normalized power density by the ratio

$$P(\rho,\phi)=|E_z(\rho,\phi)|^2/E_{\text{ref}}^2$$

where

$$E_{\text{ref}}=(E_0/N)\sum_{n=0}^{N-1}\Delta_n$$

is a convenient reference field magnitude.

III. Presentation of Results

For illustrative purposes, we choose an operating frequency of 915 MHz, cylinder radius $a=6.0$ cm, target conductivity $\sigma=1.28$ s/m, and a relative permittivity $\epsilon/\epsilon_0=51$. These latter two parameters are typical of biological materials such as human muscle [2]. We now easily deduce that $|\gamma a|=7.5$ and $\arg(\gamma a)=76.9°$.

We first of all consider the symmetrical situation where all N apertures are excited in phase with equal amplitude, i.e., $\delta_n=0$ and $\Delta_n=1$. In this case, the primary focus of the array is at the center $\rho=0$, so we really need to show only the variation of the normalized local power P as a function of the normalized radial distance ρ/a from 0 to 1.0. Such results are shown in Fig. 1 for the three cases where the number N of apertures is 4, 8, and 16. The results show that local power dissipation is quite significant at both the center of the target and at the periphery. Of particular importance is the fact that the $N=4$ aperture case has a larger power dissipation in the region between $\rho/a=0.5$ and 0.9. As N increases, we see that power levels are virtually unchanged near the center of the target but the power in the outer region has reduced levels at least along the radial $\phi=0^0$.

TABLE I
Values of δ_n in Degrees

n	N = 4	N = 8	N = 16
0	- 170.0	178.5	174.7
1	42.5	-97.2	-158.4
2	-152.1	61.4	-92.5
3	42.5	-171.5	-12.4
4		-153.1	65.6
5		-171.5	138.2
6		61.4	-167.6
7		-97.2	-149.7
8			-154.6
9			-149.7
10			-167.7
11			138.2
12			65.6
13			-12.4
14			-92.5
15			-158.4

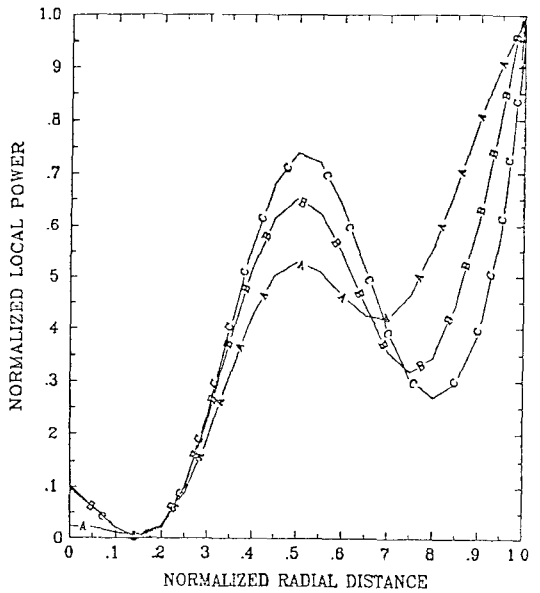

Fig. 2. Local power dissipation for the array focused at $\rho=\rho_f=0.5a$ as a function of the radial coordinate for $\phi=0^0$, where the A, B, and C curves correspond to $N=4$, 8, and 16, respectively.

To illustrate the control of the focusing, we select the phase δ_n such that the phase of the signal $E_{z,n}(\rho_f,0)$ for each value of n is the same. The prescription for doing this is spelled out explicitly in Part I. In other words, we are focusing the array of horn apertures to the point $\rho=\rho_f$ at $\phi=0^0$. Of course, it is always possible that other foci, so defined, will exist. We can call these secondary "hot spots." In the present case, we choose the amplitude factors $\Delta_n=1.0$ for all n. Furthermore, in order to show a concrete example, we specify that $\rho_f/a=0.5$. The values of δ_n, expressed in degrees, for $N=4$, 8, and 16, are listed in Table I.

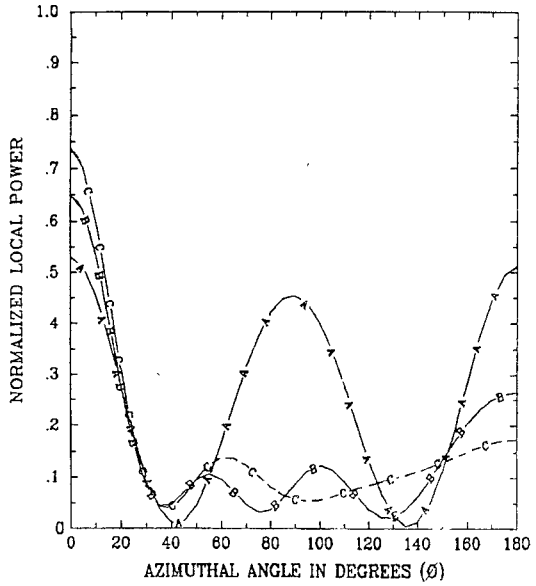

Fig. 3 Local power dissipation for the array focused at $\rho = \rho_f = 0.5a$ as a function of the azimuthal coordinate for $\rho = 0.5$ a, where the A, B, and C curves correspond to $N = 4$, 8, 16, respectively (Note that curve C does not show the details of the ripples, see text.)

Using the values of δ_n indicated above, the normalized local power P is shown plotted in Fig. 2 as a function of the normalized radial distance ρ/a for $\phi = 0^0$ for the three cases $N = 4$, 8, 16. As indicated, there is a significant enhancement of the power dissipation in the region of the focus point $\rho_f/a = 0.5$. Furthermore, the focus is most pronounced for the case of $N = 16$. To give some idea of the azimuthal variation of the power levels, P is plotted in Fig. 3 for the same condition, as a function of the angle ϕ, and for fixed $\rho/a = 0.5$. Here, we see rather dramatically that there are noticeable secondary "hot spots" for the $N = 4$ case at the 90^0 points. On the other hand, for the $N = 8$ and $N = 16$ cases, the secondary maxima do not appear. Not surprisingly, we see that the ripples in the azimuthal variation become greater in number as N increases. (Actually this detail is not evident in Fig. 3 for the $N = 16$ case because of computational limitations.)

IV. Concluding Remarks

The limitations for controlling the local power dissipation in a cylindrical target are rather severe. We have attempted to illustrate the problem with a two-dimensional model consisting of a concentric aperture array system with a prescribed form of excitation. It is confirmed that some power enhancement takes place at the focus point, but care must be taken to account for secondary foci where additional "hot spots" may occur. The latter will occur when the number of aperture elements in the array are insufficient and/or the electrical size of the cylinder is large, such that significant phase interference occurs between the individual aperture contributions at other than the desired focus point. Further investigations that deal with the aperture design problem are underway. One possible scheme is to modify the relative amplitude factors Δ_n of the individual apertures to reduce the spurious "hot spots," but care must be taken not to accomplish this at the expense of greater heating of the peripheral regions of the target. It would also be useful to extend the present numerical scheme to three-dimensional models (i.e., the axially-bounded aperture for layered cylindrical models) such as treated by Ho, Guy, Sigelmann, and Lehman [3]. These investigators, however, did not explicitly consider focusing.

Acknowledgment

The authors would like to thank Dr. T. Cetas of the University Health Sciences Center for his help and encouragement. The comments from Dr. D. G. Dudley are also appreciated.

References

[1] J. R. Wait, "Focused heating in cylindrical targets," *IEEE Trans Microwave Theory Tech.*, vol. MTT-32, pp. 647–649, July 1985
[2] C C Johnson and A. W Guy, "Properties of electromagnetic waves in muscle tissue," *Proc IEEE*, vol 60, pp 692–700, Apr. 1972
[3] H S Ho, A W Guy, R A. Sigelmann, and J. F. Lehmann, "Microwave heating of simulated limbs by aperture sources," *IEEE Trans. Microwave Theory Tech.*, vol. MTT-19, pp. 224–231, Feb. 1971

Numerical Analysis of Various Configurations of Slab Lines

GIOVANNI B. STRACCA, GIUSEPPE MACCHIARELLA, AND MARCO POLITI

***Abstract*—Numerical solutions are presented for the characteristic impedance of various line structures derived from the slab line, which allow the calculation also of the even and odd impedance of coupled slab lines. Some approximated formulas are also derived, which match the numerical results with good precision for a large range of geometrical dimensions of the structures.**

The results presented here are compared with some formulas and numerical results available from previous technical papers.

I. Introduction

In this paper, both numerical solutions and analytical interpolating formulas are presented for the characteristic impedance of the various transmission-line structures shown in Fig. 1. The structure in Fig. 1(a) is the well-known slab line, which is composed of a cylindrical metallic rod of diameter d, placed symmetrically between two parallel ground planes AA' and BB' at a distance h. The structure of Fig. 1(b), known as the trough line, and that of Fig. 1(c) are derived from the slab line by introducing in Section CD an electric conductor plane (short circuit) (Fig. 1(b)) or a magnetic conductor plane (open circuit) (Fig. 1(c)), orthogonal to the ground planes and at a distance $c/2$ from the center of the rod.

The characteristic impedance of the structure of Fig. 1(b) is equal to the odd characteristic impedance Z_{co} of two-coupled equal slab lines (Fig. 2), separated by a distance c; in addition, the characteristic impedance of the structure in Fig. 1(c) is also equal to the even characteristic impedance Z_{ce} of the structure in Fig. 2. Both characteristic impedances of the two transmission lines of Fig. 1(b) and (c) approach the characteristic impedance Z_c of the slab line, when the distance $c/2$ is very large.

Manuscript received June 25, 1985; revised October 29, 1985
G. B Stracca and M. Politi are with the Dipartimento di Elettronica, Politecnico di Milano, Piazza Leonardo da Vinci 32, 20133 Milano, Italy.
G Macchiarella is with Centro di Studio Per le Telecomunicazioni Spaziali del CNR, Via Ponzio 34/5, 20133 Milano, Italy.
IEEE Log Number 8406852.